

Betulinic acid inhibits proliferation and triggers apoptosis in human breast cancer cells by modulating ER (α/β) and p53

Yanvit Prompoon^a, Laphatrada Yurasakpong^a, Athikhun Suwannakhan^a, Chidchanok Chawiwithaya^a, Charoonroj Chotwiwatthanakun^b, Wattana Weerachatanukul^a, Chanin Nantasenam^c, Somluk Asuvapongpatana^{a,*}

^a Department of Anatomy, Faculty of Science, Mahidol University, Bangkok 10400 Thailand

^b Academic and Curriculum Division, Nakhon Sawan Campus, Mahidol University, Nakhon Sawan 60130 Thailand

^c Streamlit Open Source, Snowflake Inc., San Mateo, CA 94402 USA

*Corresponding author, e-mail: somluk.asu@mahidol.ac.th

Received 16 Jul 2023, Accepted 28 May 2024

Available online 3 Oct 2024

ABSTRACT: Although betulinic acid (BA) has been shown to attenuate breast cancer cell lines, owing to its interaction with several signaling molecules; its potential interaction with estrogen receptors (ERs) and p53 is not fully understood. Hence, we aimed to investigate the anti-cancer effect of BA on breast cancer cells, focusing on its molecular mechanisms involving the ER and p53 signaling pathways. The cell cytotoxicity of ER-positive (MCF-7) and ER-negative (MDA-MB-231) breast cancer cells was studied using MTT assay. Apoptosis was investigated by flow cytometry and Western blot analysis. The expression levels of ER α /ER β and wt-p53/mu-p53 were studied using Western blotting. Finally, a possible interaction between BA and its molecular targets was predicted using molecular docking. Upon BA treatment, both breast cancer cell lines underwent significant cell death and inhibition of cell proliferation. Flow cytometry and Western blot analysis showed that the MCF-7 cells underwent early and late apoptosis, while MDA-MB-231 underwent both apoptosis and necrosis within 48 h. The expression levels of ER α /ER β and wt-p53/mu-p53 were significantly altered. This could be partly attributed to the activation of apoptosis and inhibition of proliferation through the p53 signaling pathway, as induced by the interaction of BA with its coupling molecules.

KEYWORDS: breast cancer, betulinic acid, estrogen receptors, wild-type and mutant p53

INTRODUCTION

Breast cancer is the most commonly occurring cancer in women worldwide and is the second leading cause of cancer-related death among women [1]. It is classified based on the overexpression of surface receptors, including estrogen receptors (ERs), progesterone receptors (PRs), and the human epidermal growth factor receptor II (Her2). ERs are a nuclear receptor family mostly found within the nucleus, while a small fraction may be found in the cytoplasm or mitochondria. There are two classes of ERs, estrogen receptor alpha (ER α) and estrogen receptor beta (ER β), encoded by different genes located on different chromosomes. Despite their genetic differences, ER α and ER β share 97% and 55% similarity in their DNA-binding and ligand-binding domains, respectively. It has been reported that approximately 70% of breast cancer express ER α , while only 30% express ER β [2]. ER α and ER β differentially contribute to cancer progression, with ER α as an oncogene and ER β as a tumor suppressor [2]. Estrogen signaling is selectively stimulated or inhibited depending on the balance of these two subtypes. It has been shown that ER α -negative breast cancer cell lines such as MDA-MB-231 and MDA-MB-435 overexpress ER β , which is highly linked to cancer growth and metastasis [3], suggesting that ER β can either promote or inhibit proliferation or metastasis in breast cancer. In addition, the regulation of tumor

suppression is also known to be dependent on the close relationship between ER α and p53 signaling pathways through their direct interaction [4]. Approximately 80% of ER α -negative breast cancer cells express wild-type p53, although it is functionally debilitated. In contrast, ER α -positive breast cancer highly exhibits mutant-type p53 [5,6]. Interestingly, patients with ER α -positive breast cancer with highly expressed wild-type p53 are resistant to chemotherapy, while ER α -negative breast cancer patients with mutant p53 are still sensitive to chemotherapy [7].

Betulinic acid (BA) is a naturally occurring pentacyclic triterpenoid (Fig. S1). It is a well-known herbal extract found in various organs of a wide variety of plant species. Numerous studies have demonstrated a wide range of pharmaceutical properties of BA, including cardioprotective, anti-inflammatory, immunomodulatory, anti-HIV, anti-angiogenic, anti-fibrotic, and, of course, anti-cancer effects [8]. BA exerts anti-cancer properties against many types of human cancers, for example, prostate, melanoma, breast, colorectal, and lung cancers [8,9], raising interest in the chemotherapeutic potential of this compound. Further studies have also shown that BA could suppress tumor angiogenesis, invasion, and cancer cell stemness [10,11]. In endometriotic cells, it has recently been shown that BA inhibits the estrogen signaling pathway, either indirectly or directly [12,13], and suppresses ER β expression while exerting minimal effect on ER α [14].

More interestingly, the effect of BA-induced apoptotic cells is modulated through p53-dependent signaling in melanoma, glioblastoma, and neuroectodermal cancer cells [15]. In breast cancer, however, the effect of BA on apoptosis and the involvement of the ER and p53 signaling pathways remains to be elucidated.

Therefore, this study was conducted to investigate whether BA could induce apoptosis and inhibit the proliferation of breast cancer cells through the ER and p53 signaling pathways.

MATERIALS AND METHODS

Cell lines and reagents

The human breast cancer cell lines, MCF-7 and MDA-MB-231, were purchased from the American Type Culture Collections (ATCC, Manassas, VA, USA). The culture medium, Dulbecco's modified Eagle's medium (DMEM), and bovine fetal calf serum (BFCS) were from Gibco (Grad Island, NY, USA). Antibiotics, streptomycin, and penicillin G were purchased from GE Health Care Life Sciences (Logan, UT, USA). The betulinic acid (purity > 98% by high-performance liquid chromatography) was from Sigma-Aldrich (Merch KGaA, Darmstadt, Germany) and dissolved in DMSO at a concentration of 5 mM. The Annexin V-fluorescein isothiocyanate (FITC) mixed with propidium iodide (PI) in an Apoptosis Detection Kit was from BD Biosciences (San Jose, CA, USA). The MTT powder (3-(4,5-Dimethylthiazol-2-yl)-2,5-diphenyltetrazolium bromide) and dimethyl sulfoxide (DMSO) were purchased from Sigma-Aldrich.

The primary antibodies were purchased from Santa Cruz Biotechnology (Santa Cruz, CA, USA): p53 (#sc126), estrogen receptor alpha (#sc-8002), estrogen receptor beta (#sc-390243); and Cell Signaling Technology Inc (Danvers, MA, USA): β -actin (#4967), Bax (#2772). The secondary antibodies were obtained from Cell Signaling Technology: the anti-rabbit IgG, HRP-linked antibody (#7074), and anti-mouse IgG, HRP-linked antibody (#7076).

Cell culture

Both cancer cell lines, MCF-7 (ER-positive cell line expressing wild-type p53) and MDA-MB-231 (ER-negative cell line expressing mutant p53 R280K), were cultured in Dulbecco's modified Eagle's medium supplemented with 10% fetal bovine serum, 100 μ g/ml of streptomycin, and 100 U/ml of penicillin at 37 °C in a humidified atmosphere containing 5% CO₂. The cells were incubated with various concentrations of BA ranging from 2.5 to 60 μ M. MCF-7 and MDA-MB-231 cells supplemented with equivalent volumes of DMSO (vehicle) were used as a negative control.

Cell viability assay

Both cells were seeded onto 96-well plates at a density of 8,000 cells/well. The cells were acclimatized at 37 °C in a humidified atmosphere containing 5% CO₂ overnight. Thereafter, the cells were treated with BA at different concentrations from 2.5 to 60 μ M for 24 and 48 h. At the indicated time points, 10 μ l of MTT (5 mg/ml dissolved in PBS, pH 7.4) was added to each well and incubated at 37 °C for 3 h. After incubation, the medium was removed, and the plates were inverted onto tissue paper at room temperature for 10 min to dry the cells. For the cell viability assay, crystal formazan solution, freshly dissolved in 100 μ l of isopropanol, was added into the cells. After several washes with PBS, the absorbance of the stained cells was measured at 430 nm using a microplate reader (Bio-Rad Laboratories, Inc., Hercules, CA, USA). All experiments were performed in triplicate, and control percentage of cell viability was calculated using the following formula: cell viability (%) = [1 - (OD test/OD control)] \times 100.

Colony formation assay

Both human breast cancer cells were seeded onto six-well tissue culture plates at a density of 1×10^3 cells/well and left overnight. The cells were treated with 10, 20, and 30 μ M of BA and allowed to further culture for 10–14 days. The culture medium was changed every other day. Next, the cells were fixed with 4% formaldehyde solution for 20 min at room temperature and subsequently stained with 0.1% crystal violet solution for 15 min. Unabsorbed crystal violet was washed out by running the cells under tap water. The tissue culture plates were completely air-dried at room temperature before being photographed. To quantify the cells, samples were dissolved with 10% acetic acid solution. A total of 100 μ l of each sample was aliquoted and then loaded onto 96-well plates, and the absorbance was measured at 595 nm.

Cell apoptotic assay

Human breast cancer cells were plated onto six-well tissue plates at a density of 4×10^5 cells/well. The cells were then incubated with specified concentrations of BA (from 10 to 30 μ M) for 24 h and 48 h. Following 48 h of exposure to BA, the cells were collected and analyzed using an Annexin V/PI Apoptosis Detection Kit. Briefly, the cells were trypsinized, washed with PBS, and resuspended in 100 μ l of buffer solution (10 mM HEPES/NaOH at pH 7.4, 140 mM NaCl, 2.5 mM CaCl₂) at a final concentration of 1×10^6 cells/ml. Then, 5 μ l of the detection kit was added to the cells and left for 15 min at room temperature in the dark. Flow cytometry was performed using the FACSria™ III system. A total of 20,000 ungated events were acquired for each sample, and the obtained data were analyzed with FACSDiva version 6.1.3 (BD Biosciences).

Western blot analysis

Both cells were incubated with BA of the same concentrations following the aforementioned conditions. The cells were lysed for 10 min on ice using a RIPA buffer with 1 mM PMSF. The cell lysates were separated into supernatants and pellets by centrifuging at $10,000 \times g$ at 4°C for 10 min. The protein concentration from the cell lysates were measured using a BCA protein assay kit (Thermo Fisher Scientific, Waltham, MA, USA). In brief, 20 μg of protein was separated in 12.5% SDS/PAGE gels and transferred to polyvinylidene difluoride membrane (EMD Millipore, Billerica, MA, USA). Non-specific protein binding was blocked using a blocking solution (5% nonfat milk in 20 mM Tris-HCl, 150 mM NaCl, 0.1% Tween-20) for 2 h at room temperature. Thereafter, the membranes were incubated with the specific primary antibodies dissolved in the blocking solution for 4°C overnight. Subsequently, the membranes were washed with TBS buffer containing 0.1% Tween-20, and incubated with the secondary antibodies at room temperature for 1 h. Immunoreactivity was developed by a chemiluminescent detection kit (Thermo Fisher Scientific, Waltham, MA, USA). The bands were visualized by a Gel Doc imaging (Alpha Innotech, San Leandro, CA, USA). The intensity of immunoreactive bands was semi-quantitated by a PhosphorImager software.

Molecular docking

The possible interactions between BA and ER α , ER β , mutant-type p53, and wild-type p53 were checked using the CB-Dock software [16]. Information from the Protein Data Bank (PDB) of the studied proteins was accessed via the National Institute of Health (Bethesda, MD, USA) and was as follows: ER α (PDB#1A52), ER β (PDB#5TOA), wild-type p53 (PDB#8F2H), and mutant-p53 (PDB#6FF9); all of which belong to *Homo sapiens* sp. After docking, the model structures of the given proteins interacted with BA (displayed as either space-filling, ribbon, or ball and stick model) were superimposed. The root-mean-square distances (RMSD) of the interaction and the AutoDock score (representing a binding affinity) were calculated using PyMOL (Version 1.8).

Statistical analysis

All statistical analyses were performed by GraphPad Prism version 8.0 software (GraphPad Software, Inc., La Jolla, CA, USA). All results are presented as the mean \pm SEM calculated from three-independent experiments. Comparison between control, BA treatment, as well as positive control groups was performed by multiple comparisons via ANOVAs with Dunnett's post-hoc tests. The different levels of significance were denoted by (*) when $p < 0.05$, by (**) when $p < 0.01$ (highly significant), or by (***) when $p < 0.001$ (extremely significant).

RESULTS

Effect of BA on human breast cancer cell viability

As shown in Fig. 1, BA effectively decreased the cell viability of both breast cancer cell lines in a dose- and time-dependent manner. After BA treatment, the cell viability of MCF-7 and MDA-MB-231 significantly reduced as early as the minimal concentration of 2.5 μM BA at both 24 and 48 h, suggesting that the compound is highly effective in attacking both cancer cell types. In fact, higher concentrations of BA (up to 60 μM) did not show more substantial deterioration effect toward cancer cells; the cell viability slightly declined with the differences in cell death, not more than 10% (particularly from 10 to 60 μM).

Analysis of the minimal inhibitory concentration (IC₅₀; indicating the number of cell death of 50% upon BA treatment) revealed 14.08 and 9.03 μM for the MCF-7 cells at 24 and 48 h post-BA treatment, respectively. The values were 19.16 and 14.56 μM (at 24 and 48 h, respectively) for the MDA-MB-231 cells.

Effects of BA on colony formation in human breast cancer cells

To determine the long-term anti-cancer effect of BA against cell proliferation in both human breast cancer cell lines, a colony formation assay was performed across a 10-day period. As shown in Fig. 2A, the MCF-7 cells, representing the early stage of breast cancer, showed a significant reduction in colony formation compared with the control group. The control percentages of colony staining intensity were reduced to 56.89%, 26.74%, and 8.56% at BA concentrations of 10, 20, and 30 μM , respectively. Meanwhile, the reduction percentages of colony staining intensity in the MDA-MB-231 cells (the late-stage breast cancer cells) were 59.82%, 53.12%, and 13.25%, respectively at the three given BA concentrations, which were much lower than those of the former group (Fig. 2B).

BA-induced apoptosis in both MCF7 and MDA-MB-231 cells

Apoptosis of MCF-7 and MDA-MB-231 cells was investigated by Annexin V-FITC/PI double staining followed by a flow cytometric assay. The proportion of MCF-7 cells undergoing apoptosis significantly increased ($p < 0.001$) after 48 h of treatment with BA. Among the apoptotic population, the early apoptotic cells apparently increased to 33.5%, 46.1%, and 30.0%, while the late apoptotic cells moderately increased to 8.7%, 9.2%, and 12.5% at 10, 20, and 30 μM of BA, respectively (Fig. 3A). The positive control, where fulvestrant (targeting ER α -positive cancer) was used to treat the MCF-7 cells, induced early and late apoptotic cells by 68.8% and 12.4%, respectively.

In the MDA-MB-231 cells, apoptotic percentages of approximately 23.5% and 25.2% for early apoptosis were revealed when treated with 10 and 20 μM of BA,

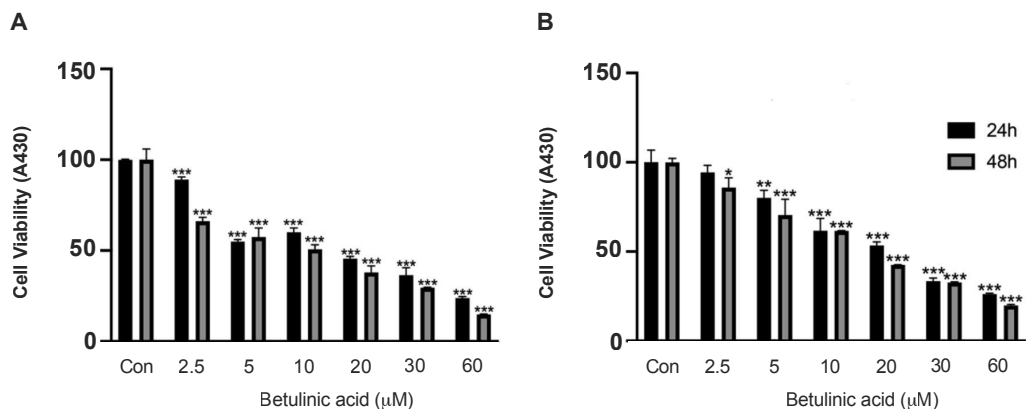


Fig. 1 MTT assay demonstrating the cytotoxic effect of BA at 24 and 48 h against MCF-7 (A) and MDA-MB-231 (B) human breast cancer cells at 24 h (solid bars) and 48 h (gray bars). The BA concentrations used in this study ranged from 2.5 to 60 μM . The results are presented as the mean \pm standard error of the mean (SEM), calculated from three-independent experiments. Statistical significance was determined by one-way ANOVAs and Dunnett's post-hoc tests, where *, **, and *** indicate $p < 0.05$ – 0.001 .

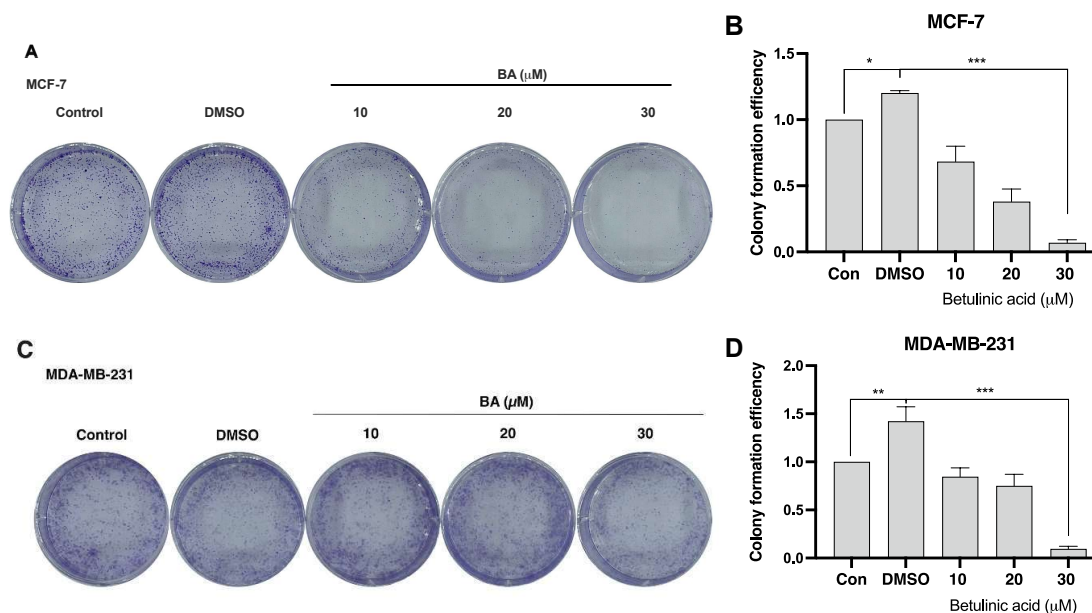


Fig. 2 Colony formation of cancer cells, MCF-7 (A) and MDA-MB-231 (B), following BA treatment and their corresponding densitometric analysis (right panels). The results are expressed as the mean \pm standard error of the mean (SEM) of three experimental repeats. One-way ANOVAs and Dunnett's post-hoc tests were performed to test statistical significance, where ** and *** indicate $p < 0.01$ – 0.001 .

respectively, while 15.3% and 13.7% were revealed for late apoptosis. However, the induction of apoptosis at the highest dose (30 μM) of BA was rather low and negligible in contrast to the percentage of necrotic cells, which was relatively high-approaching 14.8%. Interestingly, treatment with 10 μM of docetaxel (a well-known therapeutic agent for aggressive cancer such as MDA-MB-231) greatly promoted both early (34.8%) and late apoptosis (17.2%) (Fig. 3B).

These data indicate that the anti-cancer effect of BA on both human breast cancer cell lines, MCF-7 and MDA-MB-231, was modulated through the induction of apoptosis.

Changes in apoptotic markers in cancer cells followed BA induction

We further checked the alteration of protein expressions related to ER and apoptotic signaling in BA-

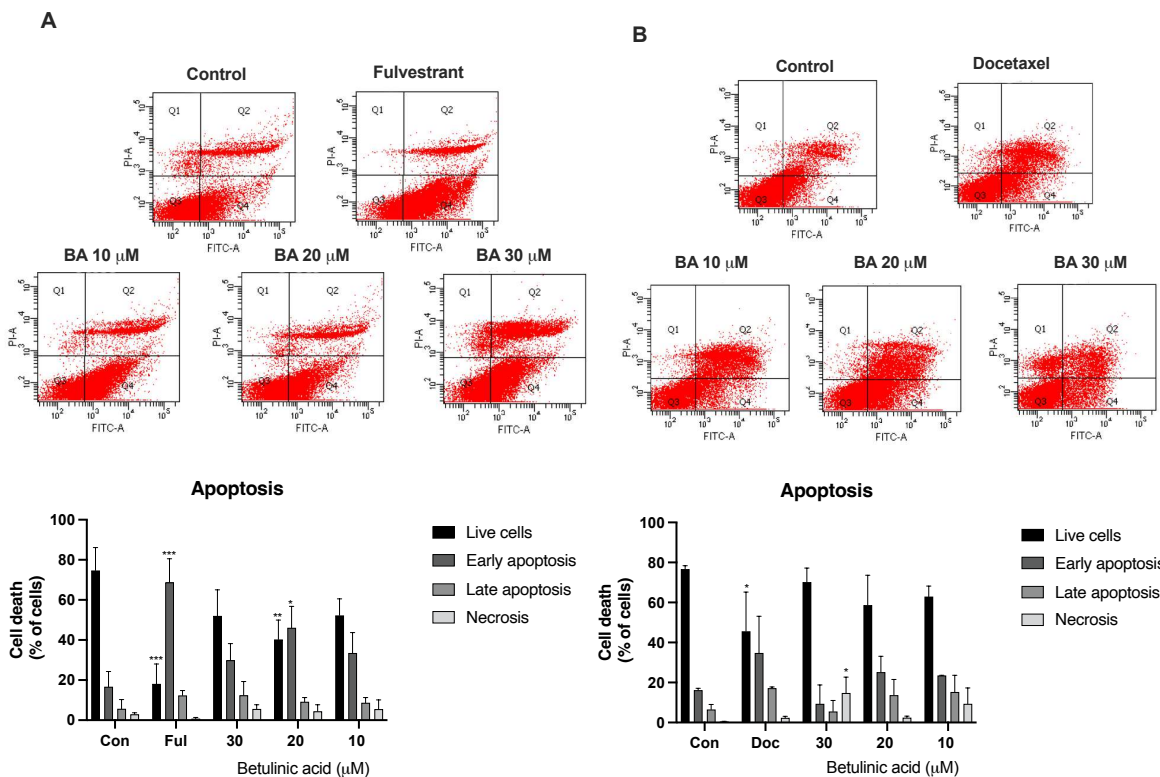


Fig. 3 Representative flow cytometric analysis of Annexin V-FITC/PI double staining in MCF-7 (A) and MDA-MB-231 (B) cancer cells at 48 h. The bar graphs in the bottom-right quadrant of each panel were created from three-independent experiments. One-way ANOVAs and Dunnett’s post-hoc tests were performed to test statistical significance, where asterisks indicated statistical significance at $p < 0.05$ – 0.001 .

treated cancer cell lines using Western blot analysis. In general, the two well-known intra-mitochondrial apoptotic markers, Bax (reactive at 20 kDa) and Bcl-xl (reactive as a doublet at 26 kDa), were apparently altered when MCF-7 and MDA-MB-231 cells were treated with BA (Fig. 4A,B). Densitometric analysis of the reactive bands indicated that the changes of the two apoptotic markers were BA concentration-dependent where Bax showed an increased trend change, while Bcl-xl showed a decreased trend change (Fig. 4A,B, right panels). In both cancer cells, the most apparent increase in Bax level was notable at 30 μM BA concentration. A significant decrease in Bcl-xl was also observed at 10 μM BA in the MCF-7 cells ($p < 0.001$), while the greatest change in MDA-MB231 could be noted at 30 μM BA. These changes corresponded to the changes seen in their positive control counterparts, particularly that of docetaxel, which was used to treat MDA-MB-231.

BA affected the expressions of ERα and ERβ

For detecting ERα and ERβ, monoclonal antibodies against these two ER forms were used, and their reactivity was recognized by the intense bands at

48 kDa (for ERα) and 56 kDa (for ERβ), respectively (Fig. 5A,B). As expected, a strong immunoreactivity toward ERα was revealed in the non-treated MCF-7 cells, which are known to engage a considerable amount of ERα (Fig. 5A, left panel, control lane). In fact, a weak-to-moderate immunoreactivity of ERα (48 kDa) was also detected in the MDA-MB-231 cells (Fig. 5B), suggesting the possible reminiscence of ERα to a variable degree in this cancer cell type. For ERβ, its expression level in MCF-7 was rather low, and only a faint staining of its immunoreactive band at 56 kDa was noted; while its expression in DMA-MB-231 was clearly recognizable (Fig. 5A,B).

Upon treating the cells with BA, the expression levels of ERα in MCF-7 and MDA-MB-231 significantly decreased in all BA concentrations, particularly in the highest one of 30 μM. This inhibitory effect of BA on MCF-7 corresponded well to the effect of fulvestrant, where its suppression on ERα was highly significant ($p < 0.001$) compared with the control group (Fig. 5A). Similarly, the expression levels of ERβ in MCF-7 and MDA-MB-231 also showed a significant decrease ($p < 0.001$) at 30 μM of BA, which was comparable to that of the docetaxel-treated group

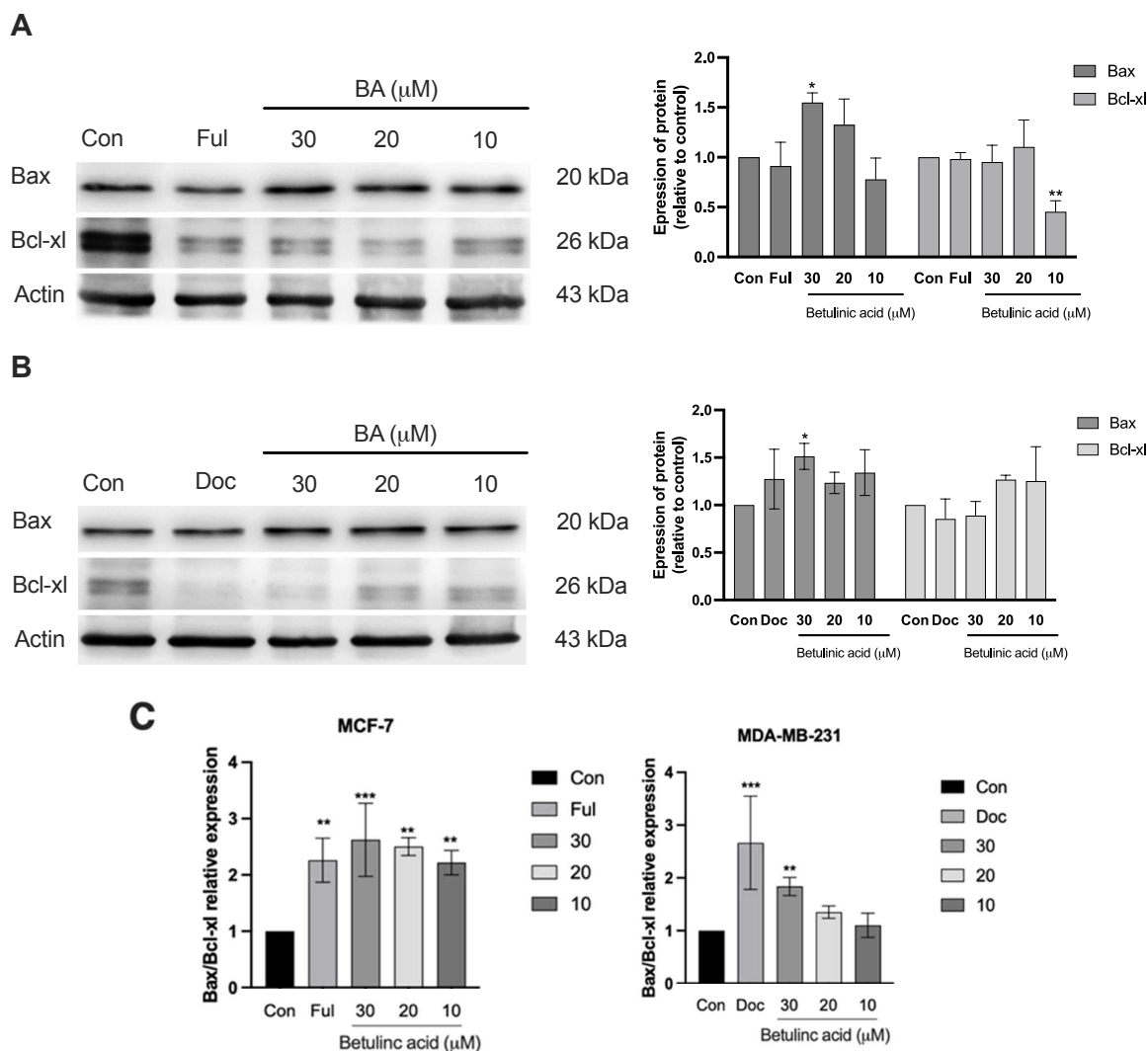


Fig. 4 Western blot analysis showing the expression of two apoptotic markers, Bax and Bcl-xl, in: (A), MCF-7; and (B), MDA-MB-231 human breast cancer cells at 48 h after BA treatment. (C), Relative expression of Bax/ Bcl-xl in MCF-7 and MDA-MB-231. Actin was used as the internal control. The results were obtained from three-independent experiments and are presented as the mean \pm stand error of the mean (SEM). The statistical significance among the groups of experiments was checked by one-way ANOVAs and Dunnett's post-hoc tests, where * and ** indicate $p < 0.05$ – 0.01 .

(Fig. 5B). Together, the results clearly suggest that BA has a promising effect on inhibiting the expression of ER α and ER β subtypes in both human cancer cells, which is likely related to apoptotic induction in the cancer cells.

To confirm the direct binding between BA and ER α and ER β proteins, molecular docking between these two molecules was performed. In this experiment, *Homo sapiens* ER α (PDB#1A52) and ER β (PDB#5TOA) were used. The results demonstrated that BA interacted with both ERs at different specific pocket sites. Hydrogen bonds were formed by the carbonyl group of BA binding to chains A and B of

the ER α , specifically with chain A at Tyr459, Thr460, Phe461, Leu462, Ser463, and Ser464; and chain B at Gly400, Arg412, Glu423, Asp426, Met427, Leu429, Ala430, and Ser433. Moreover, the interaction between BA and ER β was also found on both peptide chains, with chain A at Asp 326, Arg329, Leu406, Asn407, Ser409, Tyr411, Ser423, Arg424, Leu426, Ala427, and Leu430 residues; and chain B at Arg386, Glu389, and His464 residues (Fig. 7). In addition, the binding affinities of BA were approximately -6.9 (for ER α) and -7.3 kmol/mol (for ER β). The root-mean-square distances (RMSDs) were 0.037 \AA and 0.067 \AA for ER α and ER β , respectively.

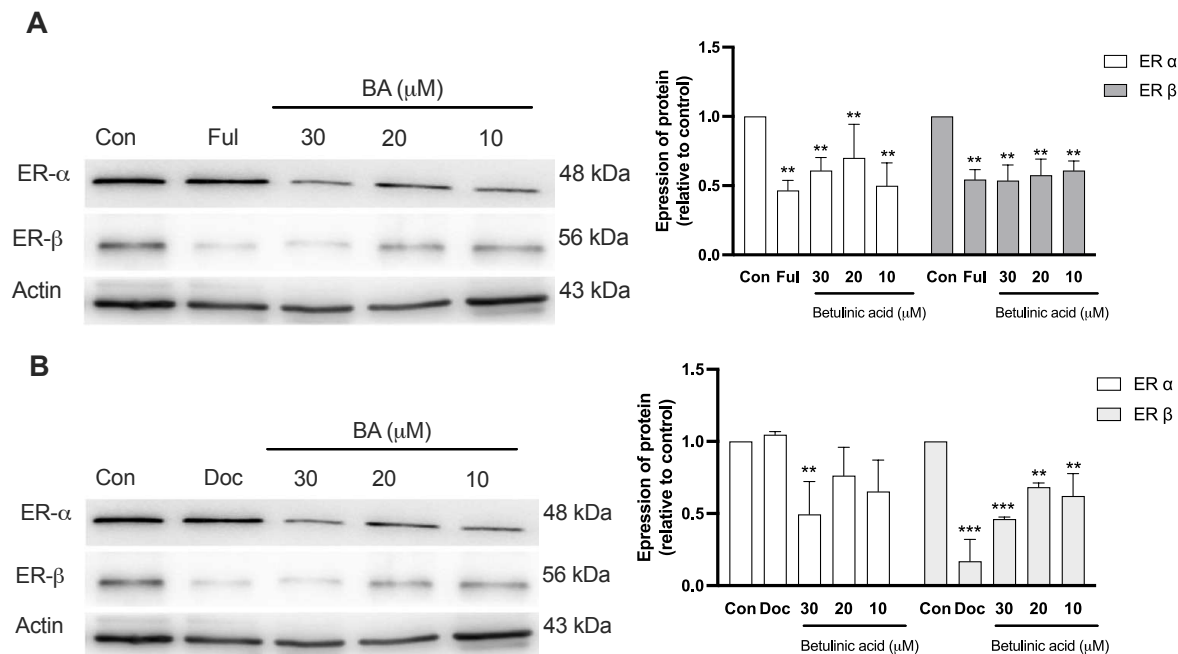


Fig. 5 Western blot analysis showing the effects of BA on the expression of ER α and ER β in: (A), MCF-7 and (B), MDA-MB-231, after 48 h of exposure. Actin was used as the internal control. The results of the densitometric analysis were obtained via three-independent experiments and are expressed as the mean \pm stand error of the mean (SEM). One-way ANOVAs and Dunnett's post-hoc tests were performed to test statistical significance, where ** and *** indicate $p < 0.01$ – 0.001 .

The expression of p53 was affected by BA treatment

We hypothesized that the BA-induced apoptosis in both cancer cell lines might be related to a direct interaction of BA and the p53 signaling molecule. Alteration in the expression of p53 was checked by Western blotting and densitometric analysis followed by molecular docking. In the non-treated cells (control), the intense reactivity of the 53-kDa protein was noted in both MCF-7 and MDA-MB-231 cancer cells (Fig. 6A,B). It is anticipated that the p53 expressed in MCF-7 is the wild-type p53 (wt-p53), and that the p53 present in MDA-MB-231 is the mutated p53 (mu-p53) [17]. The effect of BA on the expression of p53 in these two cancer cells represented the changes of these two isoforms. In the BA-treated MCF-7 cells (Fig. 6A), the expression level of wt-p53 rather fluctuated, in which its level at 10 μ M BA was apparently increased more than the control ($p < 0.001$). However, at higher concentrations, the levels of p53 significantly decreased, particularly at 30 μ M BA ($p < 0.001$). Fulvestrant treatment on the MCF-7 cells (positive control) had a decreasing trend in p53 expression, yet a significant difference was not observed. Similarly, in MDA-MB-231, the 53 kDa mu-p53 significantly decreased after treatment with BA, particularly at 30 μ M (Fig. 6B). Docetaxol treatment (positive control) significantly increased the level of mu-p53. Together, these data suggest that BA

modulates the expression levels of wt-p53 and mu-p53 in MCF-7 and MDA-MB-231 cells, respectively.

The results demonstrated that BA could interact with both ERs at different specific pocket sites (Fig. 7A–D). The possible interactions between BA and the wt-p53 and the mu-p53 were evaluated by molecular docking. The dimer structures of *Homo sapiens* wt-p53 (PDB#8F2H) and mu-p53 (PDB#6FF9) were used for the investigation. The results indicated that BA could bind to both types of p53 in different regions (Fig. 7). The carbonyl group of BA could form hydrogen bonds with the side chain B of wt-p53 at Trp23, Lys24, Pro27, Glu28, Asn29, Asn30, Ser33, Pro34, Leu188, Leu201, Arg202, Val203, and Glu204 (Fig. 7E–H). The AutoDock Vina Score (representing the binding affinity) between BA and wt-p53 was -8.5 kmol/mol. The RMSD was 0.037 Å. For mu-p53, BA formed hydrogen bonds on both side chains: chain A at Glu180, Arg181, Cys182, Ser185, Gly187, Leu188, Ala189, and Pro191; and chain B at Arg110, Leu111, Gly112, Phe113, His115, Tyr126, Pro128, and Trp146. The binding affinity of BA with mu-p53 was -9.2 kmol/mol, and the RMSD was 0.007 Å. These results suggested that BA could bind to both wt-p53 and mu-p53, and the interaction between BA and mu-p53 was plausibly stronger.

The molecular docking information was also compared between BA and fulvestrant (known ER in-

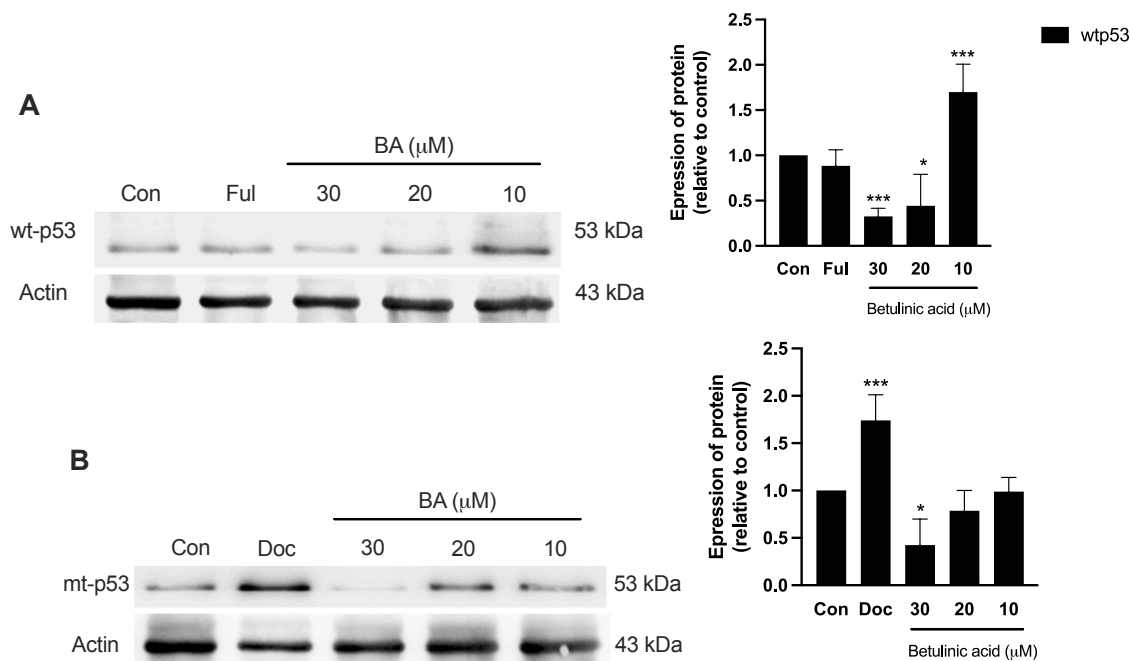


Fig. 6 Western blot analysis showing the effects of BA on the expressions of wt-p53 and mu-p53 in: (A), MCF-7 and (B), MDA-MB-231 cancer cells. Densitometric analysis (right-most panels) of the 53 kDa band was analyzed through three-independent experiments, in reference to the intensity of the actin band (as internal control) and presented as the mean \pm stand error of the mean (SEM). One-way ANOVAs and Dunnett's post-hoc tests were performed to test statistical significance, where asterisks represent $p < 0.5$ – 0.001 vs. the control.

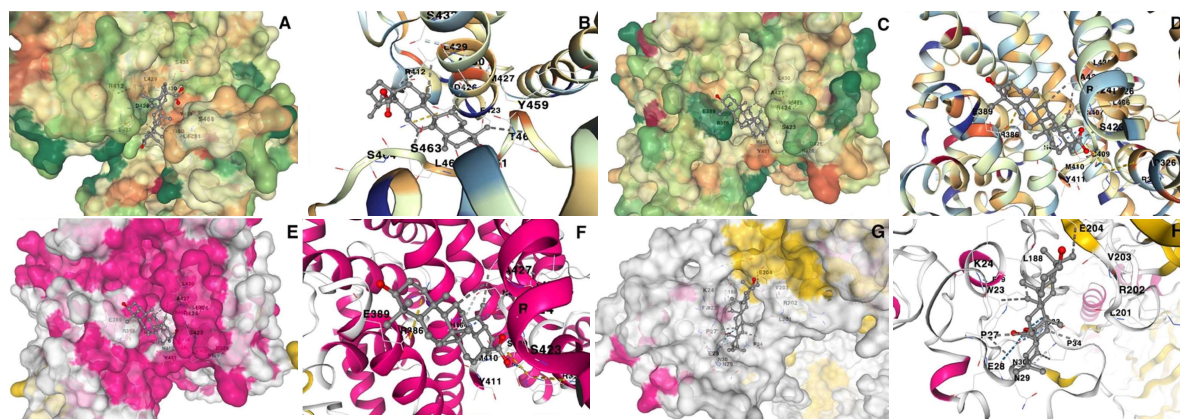


Fig. 7 Three-dimensional models of ER α (PDB#1A52) and ER β (PDB#5TOA) and molecular docking of BA into their binding cavities. A space-filling presentation (A,C) and a close-up view of the binding pockets shown in the ribbon model (for ER) and the ball and stick model (for BA) (B,D). A space-filling model (E,F) and a close-up view (G,H) of the binding pockets shown in the ribbon model (for p53) and a ball and stick model (for BA).

hibitor) and APR246 (known p53 inhibitor). We found that fulvestrant could interact with both ER subtypes only in chain B (Fig. S2) and involved almost the same residues as the BA–ER interaction. Similarly, APR246 could bind to both p53 subtypes (Fig. S3) within the similar amino acid clusters as those shown for BA interaction.

The binding potentials between fulvestrant (ER

inhibitor) and BA with *H. sapiens* ER α (PDB#1A52) and ER β (PDB#5TOA) were demonstrated. The docking results showed that fulvestrant could interact with both types of ER in distinct specific pocket regions. Hydrogen bonds were formed between fulvestrant and chain B of ER α (Fig. S2A–D). The binding affinity of fulvestrant with ER α and ER β was -7.3 and -8 kJ/mol, respectively. The root RMSDs of fulvestrant with

ER α and ER β were 2.951 Å and 2.753 Å, respectively.

In case of BA, it could bind with ER α and ER β on both side chains A and B with a binding affinity of around -7.2 and -8.2 kJ/mol (Table S1). On the chain B of ER α , the binding of BA involved similar amino acid residues as demonstrated for fulvestrant, suggesting that BA and fulvestrant might bind in the same pocket (Fig. S2F). On the chain B of ER β , close binding amino acid residues of BA were Arg386, Glu389, and His464 comparable to those of fulvestrant (Fig. S2D).

Possibility of interaction between wild-type *H. sapiens* p53 (PDB#8F2H) and mutant-type p53 (PDB#6FF9; mutated at R280K which is the same location as in MDA-MB-231 cells) with APR246 were also evaluated in comparison to BA (Fig. S3). The results demonstrated that the APR246 could bind to wild-type p53 only on chain B. Binding affinity and RMSD between wild-type p53 and APR246 were -5.1 kJ/mol and 1.246 Å, respectively (Table S1). Moreover, APR246 also interacted with mutant-type p53 at both side chains. Its binding affinity and the RMSD were -5.0 kJ/mol and 1.233 Å (Table S1). For BA, it could bind to both types of p53 in the similar manner as APR246 with the binding affinity and RMSD of -8.5 kJ/mol and 0.037 Å for wild-type p53 and -9.2 kJ/mol and 0.007 Å (for mutant-type p53) (Table S1).

DISCUSSION

This study reported the inhibitory effect of BA in breast cancer cells through its interaction with both subtypes of ER and p53, which was an induction of apoptosis of breast cancer cell lines (through MTT assay and flow cytometry; Figs. 1 and 3). Furthermore, BA also had high potency to inhibit long-term cancer cell growth (shown by colony formation assay; Fig. 2). This information demonstrated that BA is a promising alternative therapeutic agent for curing multiple types of cancer, although additional studies remain to be investigated. In fact, the multi-potency of BA in halting growth across many cancer serotypes has long been demonstrated [8, 9, 18, 19]. Recently, it had been reported that human ovarian cancer, OVCAR-8, could be inhibited by naturally extracted BA from *Mimosa caesalpiniiifolia* [20]. Similarly, BA isolated from *Physocarpus intermedius* possessed excellent cytotoxicity against ovarian carcinoma cell line SK-OV-3 [21]. As mentioned earlier, the anti-cancer effect of BA (from either herbal extraction or commercial sources) were investigated in a broad spectrum of human cancer subtypes, including prostate, melanoma, colorectal, and lung cancer. In the case of breast cancer, BA convincingly suppressed the proliferation of both BT474 (ER-positive) and MDA-MB-453 (ER-negative) breast cancer cell lines and promoted apoptotic activity in these cells [22]. The results were similar to our find-

ings, i.e., BA could attenuate proliferation and induce apoptosis in both MCF-7 (ER-positive) and MDA-MB-231 (ER-negative) breast cancer cells. Therefore, it is reasonable to assume that BA has versatile disciplinary modes to attack cancer cells through many signaling pathways with minimal effect on normal human cells [23, 24]. A previous study by Cai et al [25] revealed that BA exerted negligible effects on the normal mammary epithelial cell line MCF-10A, highlighting BA's selective cytotoxicity towards cancer cells. Hence, BA was considered a more versatile and safer therapeutic agent than existing curative agents such as fulvestrant and docetaxel (used as positive controls in this study).

To contextualize our findings, a comparison investigation was made against previous studies with comparable experimental conditions. We observed that BA exhibited significantly higher cytotoxicity towards MCF-7 cells than fulvestrant, a known MCF-7 inhibitor. For instance, a study by Tohkayomatee et al [26] demonstrated that a 48-hour treatment of 50 μ M fulvestrant resulted in an approximate 20% reduction of MCF-7 cell viability. In contrast, our findings revealed that a lower dose of BA (30 μ M) led to a substantial decrease in cell viability by over 60%, underscoring BA's superior efficacy. Moreover, BA's cytotoxicity against breast cancer cells was found to be markedly greater than that of docetaxel, a comparison based on similar experimental conditions. According to Fite et al [27], docetaxel achieved an IC₅₀ of 17.4 μ M and 24.8 μ M against MCF-7 and MDA-MB-231 cell lines, respectively. Conversely, BA demonstrated a lower IC₅₀, indicating higher potency, at 9.03 μ M for MCF-7 and 15.46 μ M for MDA-MB-231. Based on key physicochemical parameters, BA demonstrated a significant promise as a pharmacological candidate, largely conforming to Lipinski's Rule of Five, which predicated its potential for favorable oral bioavailability. Specifically, BA's molecular architecture suggested an optimal number of hydrogen bond donors and acceptors, a molecular weight under the threshold of 500 daltons (456.7 daltons), and a log *p*-value indicative of a balanced lipophilicity and hydrophilicity, essential for effective gastrointestinal absorption. This adherence to the established criteria, coupled with its selective cytotoxicity towards malignant cells over normal tissue, highlighted BA's potential efficacy and safety profile as a therapeutic agent.

The ratio of ER α and ER β in breast cancer (as also shown herein in MCF-7 cells) is associated with multiple signaling mechanisms that directly control cell proliferation and endocrine treatment response [28]. BA treatment attenuated the ER-positive cancer cells (MCF-7) through early and late apoptosis, as gauged from Annexin V/PI staining and flow cytometry (Fig. 3). This finding was in the same fashion as other ER-positive or hormone-dependent cancer cells [29]. We believe that the underlying

ing molecular mechanism of cancer cell apoptosis in this case should be ER-dependent apoptosis, which was reported for fulvestrant [26]. It is well known that ER α and its downstream signaling cascades, PI3K/AKT/mTOR [30], were involved in both intrinsic and extrinsic apoptotic pathways. Therefore, suppressing the level of ER α (induced by BA) would directly trigger cellular apoptosis, which was evidenced herein by the alteration of at least two important apoptotic markers, Bcl-xl (downregulated) and BAX (upregulated) (Fig. 4). Likewise, many recent studies reported that BA had an ability to increase pro-apoptotic Bax and Bcl-1 in melanoma, neuroblastoma, glioblastoma, colorectal carcinoma, and prostate cancer [9, 19, 31]. Apart from ER α , BA also interacted with ER β , as demonstrated by molecular docking (Fig. 7), at different ligand binding cavities. As ER α contains Leu384 and Met421, which are replaced by Met336 and Ile373 in ER β [32]; the interaction might directly suppress ER β expression, leading to endometriotic cells and subsequently resulting in the inhibition of cell growth and proliferation [14]. Knocking down the ER and p53 subtypes before BA administration to seek further functional interaction was considerably difficult due to their cross-induction/suppression during cancer progression, as mentioned above. Altering the level of ERs or p53 triggered the apoptosis of breast cancer cells through many known signaling pathways [9] even prior to BA treatment. It should also be mentioned that BA interacts with molecular chaperones such as HSP70 [9], which is structurally similar to HSP78 (or GRP78), known to modulate cellular apoptosis via endoplasmic reticular stress [33].

The broad functionality of BA toward many cancer types (particularly across ER-positive and ER-negative) is two-fold: variation in BA receptors versus broad BA reactivity toward many signaling molecules. In the former, the expression of both ER α and ER β subtypes has been demonstrated in ER α -positive (MCF-7, T-47D, and ZR-75-1) and ER α -negative (MDA-MB-231, SK-ER-3, HCC1954, and MDA-MB-453) cancer cell lines [34]. More specifically, ER α -positive and -negative breast cancer cell lines expressed ER α mRNA and protein species; for instance, MCF-7 and T47D cells expressed ER α Δ 3, Δ 5, and Δ 7 spliced variants; while MDA-MB-231 and HCC1954 cells expressed ER α Δ 5 and Δ 7 spliced variants. In addition, all breast cancer cell lines expressed ER β 1, while ER β 2 was only present in some ER α -positive and -negative breast cancer cells [34]. In the latter, BA was shown to interact and modulate many signaling molecules and their cascades such as GRP78 [25], NF- κ B [35], and HSP70 [9]. In our case, we found that BA altered the expression of the p53 signaling protein, which is known to be involved in cell proliferation and induction of apoptosis [36]. A similar effect of BA on inhibiting the proliferation of melanoma cells through

induction of p53 was also reported [37]. It should also be mentioned that the altered p53 protein in MCF-7 was presumably the wild-type form (wt-p53), while MDA-MB-231 cells harbored a mutant p53 [17]. Accumulation of wt-p53 protein was detected after BA treatment in neuroblastoma cells, while BA was highly sensitive and related to the loss of wt-p53 function in mu-p53 medulloblastoma cells and HT-29 colon carcinoma cells [15, 38]. A recent study in prostate cancer cells also demonstrated that BA inhibited proliferation and induced apoptosis by stabilizing wt-p53 in LNCaP cells and mu-p53 in DU145 cells [39]. In fact, our molecular docking results provided further insights into the interaction between BA and p53 protein (Fig. 7). While crosstalk between ER α and wt-p53 was known to play a vital role in the progression of many cancer types [40], the interaction between ER β and mu-p53 altered by BA remained unclear and needed further elucidation. Molecular docking analyses were also conducted on recognized inhibitors, specifically fulvestrant for ER (Fig. S2) and APR246 for p53 (Fig. S3), to facilitate comparative evaluation, utilizing crystal structures from *Homo sapiens* sp. wild-type p53 (PDB#8F2H) observed in MCF-7 cells, and mutant-type p53 (PDB#6FF9) with an R280K mutation found in MDA-MB-231 cells. The findings revealed that both BA and APR246 could bind to different regions of both wild-type and mutant-type p53 proteins. APR246 showed a specific affinity for chain B of wild-type p53, whereas it interacted with both chains A and B of the mutant-type p53. Notably, BA demonstrated a higher binding affinity for wild-type p53 compared with APR246, suggesting its potential as an inhibitor of p53 function, akin to APR246. However, BA and APR246 exhibited distinct binding patterns with mutant-type p53, indicating their varied interaction mechanisms. The study highlighted the nuanced interactions of these compounds with p53 variants, underscoring the potential of BA and APR246 in modulating p53 functions, which could have implications for therapeutic strategies targeting p53 in cancer cells. We acknowledge that molecular docking simulations serve as preliminary indicators rather than conclusive evidence of direct interactions between molecules. Therefore, it is essential to pursue further experimental validation, such as immunoprecipitation, to confirm these interactions definitively.

CONCLUSION

In conclusion, our study reported the inhibitory effect of BA against breast cancer cells through its possible modulation of both subtypes of ER and p53. This resulted in a significant reduction in cell proliferation and the induction of apoptosis, which ultimately led to a marked reduction in colony formation. The functional interactions between BA, ER, wt-p53, and mt-p53, as well as cross-talk mechanisms, remained

uncertain, warranting further experimental studies. Additionally, conducting animal studies is essential to rule out the effect of BA on cellular proliferation and apoptosis through ER and p53 signaling *in vivo*. This study indicated that BA is a versatile multi-target compound that could be further developed as a therapeutic agent for breast cancer and other types of human cancer. Insights gained on the mechanisms by which BA interacts with ER and modulates the p53 signaling pathway could be valuable for the design and development of novel breast cancer therapeutic agents via the modulation of these targets.

Appendix A. Supplementary data

Supplementary data associated with this article can be found at <https://dx.doi.org/10.2306/scienceasia1513-1874.2024.085>.

Acknowledgements: The authors thank the Center of Nanoimaging (CNI) and the Central Instrument Facility (CIF), Faculty of Science, Mahidol University, for providing instrumental support throughout this work.

REFERENCES

- Giaquinto AN, Sung H, Miller KD, Kramer JL, Newman LA, Minihan A, Jemal A, Siegel RL (2022) Breast cancer statistics, 2022. *CA Cancer J Clin* **72**, 524–541.
- Wang J, Zhang C, Chen K, Tang H, Tang J, Song C, Xie X (2015) ER β 1 inversely correlates with PTEN/PI3K/AKT pathway and predicts a favorable prognosis in triple-negative breast cancer. *Breast Cancer Res* **152**, 255–269.
- Hou YF, Yuan ST, Li HC, Wu J, Lu JS, Liu G, Lu LJ, Shen ZZ, et al (2004) ER β exerts multiple stimulative effects on human breast carcinoma cells. *Oncogene* **23**, 5799–806.
- Konduri SD, Medisetty R, Liu W, Kaiparettu BA, Srivastava P, Brauch H, Fritz P, Swetzig WM, et al (2010) Mechanisms of estrogen receptor antagonism toward p53 and its implications in breast cancer therapeutic response and stem cell regulation. *Proc Natl Acad Sci USA* **107**, 15081–15086.
- Miller LD, Smeds J, George J, Vega VB, Vergara L, Ploner A, Pawitan Y, Hall P, et al (2005) An expression signature for p53 status in human breast cancer predicts mutation status, transcriptional effects, and patient survival. *Proc Natl Acad Sci USA* **102**, 13550–13555.
- Olivier M, Langerød A, Carrieri P, Bergh J, Klaar S, Eyfjord J, Theillet C, Rodriguez C, et al (2006) The clinical value of somatic TP53 gene mutations in 1,794 patients with breast cancer. *Clin Cancer Res* **12**, 1157–1167.
- Bertheau P, Lehmann-Che J, Varna M, Dumay A, Poirot B, Porcher R, Turpin E, Plassa L-F, et al (2013) p53 in breast cancer subtypes and new insights into response to chemotherapy. *The Breast* **22**, S27–S29.
- Saneja A, Arora D, Kumar R, Dubey RD, Panda AK, Gupta PN (2018) Therapeutic applications of betulinic acid nanoformulations. *Ann N Y Acad Sci* **1421**, 5–18.
- Yurasakpong L, Nantasenamat C, Nobsathian S, Chaitirayanon K, Apisawetakan S (2021) Betulinic acid modulates the expression of HSPA and activates apoptosis in two cell lines of human colorectal cancer. *Molecules* **26**, 6377.
- Jiang W, Li X, Dong S, Zhou W (2021) Betulinic acid in the treatment of tumour diseases: Application and research progress. *Biomed Pharmacother* **142**, 111990.
- Zhang DM, Xu HG, Wang L, Li YJ, Sun PH, Wu XM, Wang GJ, Chen WM, et al (2015) Betulinic acid and its derivatives as potential antitumor agents. *Med Res Rev* **35**, 1127–1155.
- Hohmann N, Xia N, Steinkamp-Fenske K, Förstermann U, Li H (2016) Estrogen receptor signaling and the PI3K/Akt pathway are involved in betulinic acid-induced eNOS activation. *Molecules* **21**, 973.
- Kim H-I, Quan F-S, Kim J-E, Lee N-R, Kim HJ, Jo SJ, Lee C-M, Jang DS, et al (2014) Inhibition of estrogen signaling through depletion of estrogen receptor alpha by ursolic acid and betulinic acid from *Prunella vulgaris* var. *lilacina*. *Biochem Biophys Res Commun* **451**, 282–287.
- Xiang D, Zhao M, Cai X, Wang Y, Zhang L, Yao H, Liu M, Yang H, et al (2020) Betulinic acid inhibits endometriosis through suppression of estrogen receptor β signaling pathway. *Front Endocrinol* **11**, 604648.
- Meng RD, El-Deiry WS (2001) p53-independent up-regulation of KILLER/DR5 TRAIL receptor expression by glucocorticoids and interferon- γ . *Exp Cell Res* **262**, 154–169.
- Liu Y, Yang X, Gan J, Chen S, Xiao Z-X, Cao Y (2022) CB-Dock2: improved protein-ligand blind docking by integrating cavity detection, docking and homologous template fitting. *Nucleic Acids Res* **50**, W159–W164.
- Hui L, Zheng Y, Yan Y, Bargonetti J, Foster DA (2006) Mutant p53 in MDA-MB-231 breast cancer cells is stabilized by elevated phospholipase D activity and contributes to survival signals generated by phospholipase D. *Oncogene* **25**, 7305–7310.
- Hsu T-I, Wang M-C, Chen S-Y, Huang S-T, Yeh Y-M, Su W-C, Chang W-C, Hung J-J (2012) Betulinic acid decreases specificity protein 1 (Sp1) level via increasing the sumoylation of sp1 to inhibit lung cancer growth. *Mol Pharmacol* **82**, 1115–1128.
- Zheng Y, Liu P, Wang N, Wang S, Yang B, Li M, Chen J, Situ H, et al (2019) Betulinic acid suppresses breast cancer metastasis by targeting GRP78-mediated glycolysis and ER stress apoptotic pathway. *Oxid Med Cell Longev* **2019**, 8781690.
- Monção NBN, Araújo BQ, Silva JDN, Lima DJB, Ferreira PMP, Airoidi FPD, Pessoa C, Citó AMdGL (2015) Assessing chemical constituents of *Mimosa caesalpiniiifolia* stem bark: possible bioactive components accountable for the cytotoxic effect of *M. caesalpiniiifolia* on human tumour cell lines. *Molecules* **20**, 4204–4224.
- Kim Y-K, Yoon SK, Ryu SY (2000) Cytotoxic triterpenes from stem bark of *Physocarpus intermedius*. *Planta Medica* **66**, 485–486.
- Liu X, Iutooru I, Lei P, Kim K, Lee S-o, Brents LK, Prather PL, Safe S (2012) Betulinic acid targets YY1 and ErbB2 through cannabinoid receptor-dependent disruption of microRNA-27a: ZBTB10 in breast cancer betulinic acid downregulates ErbB2 in breast cancer cells. *Mol Cancer Ther* **11**, 1421–1431.
- Zuco V, Supino R, Righetti SC, Cleris L, Marchesi E, Gambacorti-Passerini C, Formelli F (2002) Selective cytotoxicity of betulinic acid on tumor cell lines, but not on

- normal cells. *Cancer Lett* **175**, 17–25.
24. Yang Y, Xie T, Tian X, Han N, Liu X, Chen H, Qi J, Gao F, et al (2020) Betulinic acid-nitrogen heterocyclic derivatives: design, synthesis, and antitumor evaluation *in vitro*. *Molecules* **25**, 948.
 25. Cai Y, Zheng Y, Gu J, Wang S, Wang N, Yang B, Zhang F, Wang D, et al (2018) Betulinic acid chemosensitizes breast cancer by triggering ER stress-mediated apoptosis by directly targeting GRP78. *Cell Death Dis* **9**, 636.
 26. Tohkayomatee R, Reabroi S, Tungmunnithum D, Parichatikanond W, Pinthong D (2022) Andrographolide exhibits anticancer activity against breast cancer cells (MCF-7 and MDA-MB-231 Cells) through suppressing cell proliferation and inducing cell apoptosis via inactivation of ER- α ; receptor and PI3K/AKT/mTOR signaling. *Molecules* **27**, 3544.
 27. Fite A, Goua M, Wahle K, Schofield A, Hutcheon A, Heys S (2007) Potentiation of the anti-tumour effect of docetaxel by conjugated linoleic acids (CLAs) in breast cancer cells *in vitro*. *Prostaglandins Leukot Essent Fatty Acids* **77**, 87–96.
 28. Madeira M, Mattar A, Logullo AF, Soares FA, Gebrim LH (2013) Estrogen receptor alpha/beta ratio and estrogen receptor beta as predictors of endocrine therapy responsiveness – a randomized neoadjuvant trial comparison between anastrozole and tamoxifen for the treatment of postmenopausal breast cancer. *BMC Cancer* **13**, 425.
 29. Rieger AM, Nelson KL, Konowalchuk JD, Barreda DR (2011) Modified annexin V/propidium iodide apoptosis assay for accurate assessment of cell death. *J Vis Exp* **2011**, e2597.
 30. du Rusquec P, Blonz C, Frenel JS, Campone M (2020) Targeting the PI3K/Akt/mTOR pathway in estrogen-receptor positive HER2 negative advanced breast cancer. *Ther Adv Med Oncol* **12**, 1758835920940939.
 31. Wang X, Luo Y, Sun H, Feng J, Ma S, Liu J, Huang B (2015) Dynamic expression changes of Bcl-2, Caspase-3 and Hsp70 in middle cerebral artery occlusion rats. *Brain Injury* **29**, 93–97.
 32. Paterni I, Granchi C, Katzenellenbogen JA, Minutolo F (2014) Estrogen receptors alpha (ER α) and beta (ER β): subtype-selective ligands and clinical potential. *Steroids* **90**, 13–29.
 33. Ni M, Zhang Y, Lee AS (2011) Beyond the endoplasmic reticulum: atypical GRP78 in cell viability, signalling and therapeutic targeting. *Biochem J* **434**, 181–188.
 34. Oturkar CC, Gandhi N, Rao P, Eng KH, Miller A, Singh PK, Zsiros E, Odunsi KO, et al (2022) Estrogen receptor-beta2 (ER β 2)-mutant p53-FOXM1 axis: a novel driver of proliferation, chemoresistance, and disease progression in high grade serous ovarian cancer (HGSOC). *Cancers* **14**, 1120.
 35. Parrondo R, Pozas Adl, Reiner T, Rai P, Perez-Stable C (2010) NF- κ B activation enhances cell death by antimetabolic drugs in human prostate cancer cells. *Mol Cancer* **9**, 182.
 36. Al-Bader M, Ford C, Al-Ayadhy B, Francis I (2011) Analysis of estrogen receptor isoforms and variants in breast cancer cell lines. *Exp Ther Med* **3**, 537–544.
 37. Pisha E, Chai H, Lee IS, Chagwedera TE, Farnsworth NR, Cordell GA, Beecher CW, Fong HH, et al (1995) Discovery of betulinic acid as a selective inhibitor of human melanoma that functions by induction of apoptosis. *Nat Med* **1**, 1046–1051.
 38. Fulda S, Friesen C, Los M, Scaffidi C, Mier W, Benedict M, Nuñez G, Krammer PH, et al (1997) Betulinic acid triggers CD95 (APO-1/Fas)-and p53-independent apoptosis via activation of caspases in neuroectodermal tumors. *Cancer Res* **57**, 4956–4964.
 39. Shankar E, Zhang A, Franco D, Gupta S (2017) Betulinic acid-mediated apoptosis in human prostate cancer cells involves p53 and nuclear factor-kappa B (NF- κ B) pathways. *Molecules* **22**, 264.
 40. Walerych D, Napoli M, Collavin L, Del Sal G (2012) The rebel angel: mutant p53 as the driving oncogene in breast cancer. *Carcinogenesis* **33**, 2007–2017.

Appendix A. Supplementary data

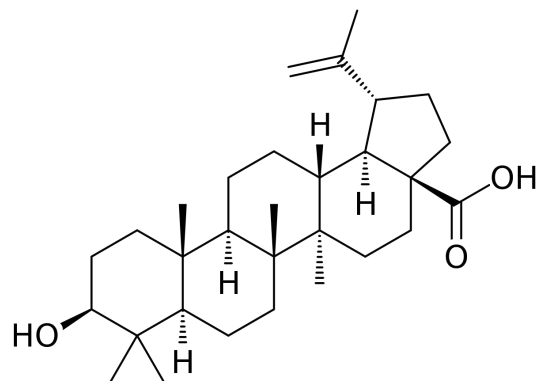


Fig. S1 The structure of the betulinic acid (BA).

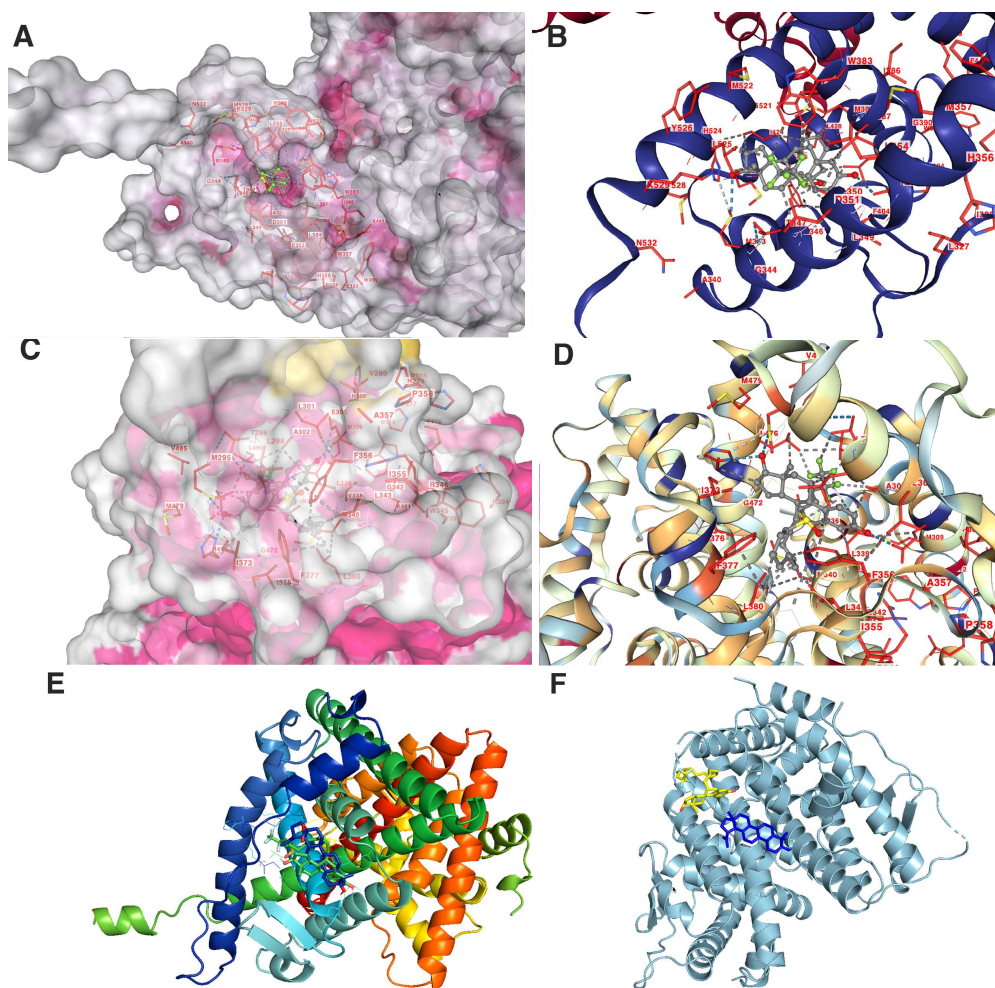


Fig. S2 Docked structure of ERα (PDB#1A52) and ERβ (PDB#5TOA) (panels A and C) indicating the binding of fulvestrant with ERα and ERβ at different regions with their close-up views (panels B and D). Comparative dockings between BA (blue) and fulvestrant (green or yellow) with ERα and ERβ are shown in panels E and F.

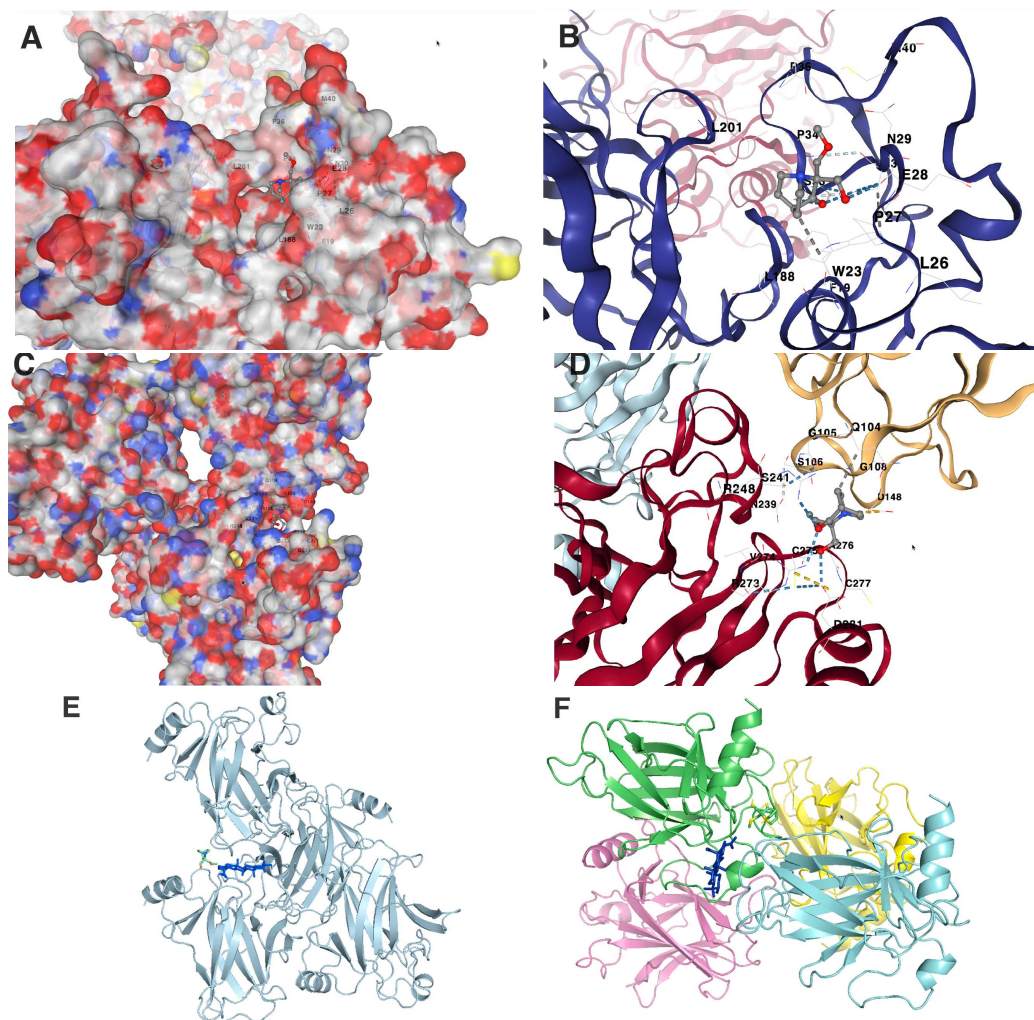


Fig. S3 Docking between the different types of p53: wide-type p53 (PDBID#8F2H) and C (PDBID#6FF9) (panels A and B) with the close-up views (panels C and D). Comparative docking of BA (blue) with wide-type p53 and wide-type p53 are shown in panels E and F.

Table S1 Summary of docking information of all studied ligands and proteins.

Name of proteins	Name of ligands	BD (kmol/mol)	RMSD (Å)
ERβ (#5TOA)	Betulinic acid	-8.2	0.037
ERα (#1A52)	Betulinic acid	-7.2	0.067
Mutant p53 (#6FF9)	Betulinic acid	-9.2	0.007
Wild p53 (#8F2H)	Betulinic acid	-8.5	0.037
ERβ (#5TOA)	Fulvestrant	14.4	2.753
ERα (#1A52)	Fulvestrant	10.8	2.951
Mutant p53 (#6FF9)	APR246	-5.0	1.233
Wild p53 (#8F2H)	APR246	-5.2	1.246